Preparation of Novel Lanthanide Complexes with Hindered Amine via Solid-State Reaction and Preliminary Evaluation of Their Efficiency as Light Stabilizers

Tao Yang, Jiachun Feng

Key Laboratory of Molecular Engineering of Polymers of Ministry of Education, Department of Macromolecular Science and Laboratory of Advanced Materials, Fudan University, Shanghai 200433, People's Republic of China

Received 23 August 2009; accepted 15 December 2009
DOI 10.1002/app.31998
Published online 2 March 2010 in Wiley InterScience (www.interscience.wiley.com).

ABSTRACT: In this research, a series of lanthanide complexes with a low molecular weight hindered amine have been synthesized for the first time from lanthanide chloride and bis-(2,2,6,6-tetramethyl-4-piperidinyl)-decanedioicacid (L) by simply using a solvent-free solid-state reaction. Elemental and thermo analysis suggest that the component of the complexes is $LnLCl_3$ $2H_2O$ (Ln = Y, La, Nd, Sm, Eu, Gd, Dy, Er). Infrared spectra indicate that the lanthanide ions are coordinated with oxygen atoms of the carbonyl group in ligand. Polypropylene films containing the ligand and complexes were prepared by melt blending and compression molding, and were exposed to UV irradiation before and after ethanol extraction. The measurements of carbonyl index, thermal decomposition temperature, and tensile elongation at break reveal that these complexes have comparable photostabilizing efficiency and improved extraction resistance compared to the ligand alone. This study suggests that hindered-amine lanthanide complexes can provide novel approach to the cheap and efficient light stabilizers. © 2010 Wiley Periodicals, Inc. J Appl Polym Sci 117: 250–258, 2010

Key words: lanthanide complexes; light stabilizer; solid-state reaction; photostabilizing efficiency; extraction resistance

INTRODUCTION

Polymer products, which are used extensively outdoors, are susceptible to degradation by ultraviolet (UV) light. Such kind of photodegradation process causes many problems, such as cracking, chalking, discoloration, and failure of physical properties of polymer.[1] A various of light stabilizers, mainly including UV absorbers and hindered-amine light stabilizers (HALS), have been developed and successfully applied to minimize these unfavorable effects of the UV light.[2] Among these light stabilizers, HALS containing piperidine is particularly interesting because of their higher photostabilizing efficiency. It has been generally believed that the dominating stabilization mechanism of HALS is through the formation of stabilizing species, nitroxyl radical and related amino ether, and their cyclic regeneration during scavenging superoxide species.[3-5] However, low molecular weight HALS often suffer from the disadvantages of high volatility at high processing temperatures and poor extraction resistance towards solvents, resulting in the decrease of photostabilizing efficiency and the contamination associated with the migrated stabilizers.[6] Earlier studies suggest that HALS with higher molecular weight can provide more resistant activity to volatility and solvent extraction by increasing their molecular weight in the range from 2000 to 3000.[7,8] In practical application, many oligomeric or polymeric HALS such as Tinuvin 944 and Tinuvin 622 have been prepared and commercialized.[9,10] These products are usually approached by complicated reactions of multifunctional organic compounds containing hindered amine group, copolymerization of monomers and HALS containing vinyl group,[11,12] or chemical modification of preformed polymer.[13,14] Such kinds of complicated chemical processes inevitably increase the environmental impact and preparation cost. Although much progress has been achieved in the preparation and application of polymeric HALS, the development of new light stabilizer with improved migration resistance via

Correspondence to: J. Feng (jcfeng@fudan.edu.cn).
Contract grant sponsor: Natural Science Foundation of China; contract grant numbers: 50673021, 20874017.
Contract grant sponsor: Shanghai-Unilever Research and Development Fund; contract grant number: 09520715500.
Contract grant sponsor: National Hi-Tech Research & Development Program; contract grant number: 2007AA03Z450.

accessible methods with less environmental impact remains an essential topic in the polymer additives research.

Recently, the rare earth compounds have attracted a great deal of attention owing to their well-defined coordination geometries, distinctive electrochemical and photochemical properties.[15-17] Some of the rare earth compounds have demonstrated stability effects in polymer and medicine field. For example, lanthanum stearate was used as an effective thermal stabilizer in PVC.[18] Cerium oxide nanoparticles were used to prevent retinal degeneration by scavenging reactive oxygen intermediates generating during photo bombardment.[19] Some complexes of lanthanide with antioxidation drugs, such as quercetin, chromones and Schiff-base, exhibited higher intrinsic binding constants with DNA and higher activity in the suppression of $O_2^{-\bullet}$ and $OH^{\bullet}$ than their ligands alone. These complexes, which were bound to DNA by either intercalation or covalent way, exhibited considerable scavenging activity due to the chelation of organic molecules to rare earth ions and the selective effects of the rare earth on scavenging radicals of the system.[20-22] We believe that the rare earth complexes with piperidine-containing HALS ligand will exhibit effective photostabilizing ability and improved migration resistance due to their relatively higher molecular weight and probably chemical interaction with preoxidized polymer chain. Currently, limited researches on the lanthanide complexes with HALS have been reported. In this article, we have synthesized a series of novel lanthanide complexes using a low molecular weight HALS as ligand for the first time, and used elemental and thermal analysis methods to characterize the chemical structures of these complexes. Their photostabilizing efficiencies and migration resistant performance were also investigated. Our results suggest that hindered-amine lanthanide complexes can provide novel approaches to the cheap and efficient light stabilizers.

EXPERIMENTAL

Materials

The commercial hindered-amine light stabilizer, Tinuvin® 770 (Bis-(2,2,6,6-tetramethyl-4-piperidinyl)-decanedioicacid) (melt pointing = 85°C), was purchased from Ciba Specialty Chemicals. Polypropylene (PP) (powder form, melt flow rate (MFR) = 0.3 g/10 min at 230°C and 2.160 kg) was kindly supplied by Yangzhou Petrochemical Co. (Yangzhou, Jiangsu province, China). Other chemicals were all reagent grade and used as received.

Tinuvin® 770 was used as ligand (**L**) and its chemical structure is shown below:

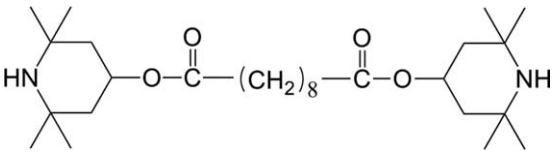

Synthesis and characterization of the complexes

Lanthanide chlorides were prepared by dissolving an appropriate weighed amount of the oxides (99.9%), Ln_2O_3 (Ln = Y, La, Nd, Sm, Eu, Gd, Dy, Er) in concentrated hydrochloric acid (d = 1.19 g/mL). The excess of the acid and water were evaporated and the residue was collected.

The lanthanide complexes were prepared using the following procedure: the mixtures of different lanthanide chloride and ligand **L** with molar ratio of 1 : 1 were put in a mortar box and ground thoroughly for 15 min at room temperature and then transferred to a 90°C vacuum oven for 120 min, followed by another 45 min of grinding at room temperature. The products were subsequently collected and excessively washed with cyclohexane and anhydrous alcohol, respectively, to remove the unreacted lanthanide chlorides or ligand. The resulting precomplexes were dried in vacuum oven at 65°C until constant weight was achieved. The final complexes were kept in a desiccator before use. The reaction process was monitored by recording the endothermic melting traces of the reaction mixture using Mettler-Toledo DSC822^e differential scanning calorimetry (DSC) from 30 to 180°C with a heating rate of 10°C/min under nitrogen atmosphere.

The complexes were characterized by Fourier transform infrared spectra (FTIR), elemental analysis, and thermal analysis. A Nicolet Nexus 470 Infrared Spectrometer was used to collect the IR spectra in the range of 4000–500 cm^{-1}. All spectra collected were averages of 32 scans with a 4 cm^{-1} resolution. The amounts of C, N, and H were determined with an Elementar Vario El III Elemental analyzer. The thermal degradation process was recorded with a Shimadzu DTG-60 thermogravimetric analyzer (TGA) in the simultaneous TGA/DTA mode from 20 to 700°C with a heating rate of 20°C/min under an oxygen flow rate of 50 mL/min.

Sample preparation for accelerated weathering and solvent-extraction tests

The PP samples were prepared using a two-step procedure; the ligand **L** and various complexes at concentration of 0.5% by weight were compounded with the PP powders by melt blending using a PLE 651 Brabender Mixer (Brabender, Germany), respectively. The temperature was kept at 175°C and the roller speed was set at 45 rpm. After a constant

value of torque was obtained, the melted mixtures were mixed for another 5 min to get a homogeneous blend. The resulting mixture were subsequently molded into 0.1-mm-thick film at 190°C in a press under a pressure of 15 MPa for 5 min and then naturally cooled down to room temperature. Here we marked the PP samples containing the ligand and the complexes of Y, La, Nd, Sm, Eu, Gd, Dy, and Er as PP/**L**, PP/Y, PP/La, PP/Nd, PP/Eu, PP/Gd, PP/Dy, and PP/Er, respectively. For comparative purpose, unstabilized neat PP sample was also subjected to the same blending and molding procedure so that it had experienced similar processing history with the samples containing stabilizers. The morphology and crystallization behavior of as-prepared samples were, respectively, studied with wide angle X-ray diffraction (WAXD, PANalytical, Netherlands) and DSC using a 10/–10/10°C/min scanning program between 20 and 210°C.

Evaluation of photostabilization and solvent-extraction resistance

To comparatively evaluate the photostabilizing efficiency of the complexes and the ligand, accelerated photodegradation of various PP films was carried out in a RW-UVC-FD1 Test Chamber (Shenzhen, China). Ten 25 W mercury lamps with wavelength range of 315–400 nm were used as the UV source. Specimens cut from 0.1-mm-thick film with about 50 mm × 20 mm in area, were mounted on racks positioned at a distance of about 10 cm from the lamps and the temperature in the cabinet was maintained at 30 ± 5°C. Irradiated specimens were collected at regular intervals to evaluate the extent of photodegradation.

Solvent extraction was performed in a Saxhlet distill apparatus. Specimens were cut into pieces of about 40 mm × 20 mm in area and extracted with 70% ethanol aqueous solution. After distilling for 48 h, the extracted specimens were dried and transferred to the UV Test Chamber for accelerated photodegradation.

The structural changes of PP samples with or without solvent extraction upon UV irradiation were investigated using FTIR spectroscopy. Carbonyl index (CI), as determined from FTIR spectra, was used to characterize the extent of degradation in PP. It was defined as the area of carbonyl absorption band related to the area of a reference band: $CI = A_C/A_R$, where A_C is the area of the carbonyl absorption band in the range from 1700 to 1800 cm^{-1}, while A_R is the area of reference band in the range from 2700 to 2750 cm^{-1} (CH bending and CH_3 stretching band). A_R used as reference was constant during the degradation processes.[23]

In addition to CI, the initial thermal decomposition temperatures of aged samples were also measured to evaluate the extent of UV degradation using DTG-60 TGA instrument under oxygen atmosphere with a heating rate of 20°C/min from 20 to 400°C. Moreover, the tensile elongation at break of neat PP, PP/L, and PP/Nd with various UV accelerated photodegradation durations was tested on a SANS CMT4104 Tensile Tester (Shenzhen, China) at 23 ± 1°C. The tensile specimens were prepared by compression molding of as-prepared samples into 0.4-mm-thick sheets at 200°C, and then punched to a dumbbell shape. The narrow portion of the dumbbell specimens was 17 mm (length) × 4.2 mm (width) × 0.40 mm (thickness) in dimension and the crosshead speed was 10 mm/min. For each sample, over three specimens were tested and the average values were used.

RESULTS AND DISCUSSION

Synthesis and characterization of the complex

The new complexes were synthesized by a simply solid-state reaction of lanthanide chlorides and ligand **L**. In contrast with conventional solution reactions, the solvent-free reaction used in this study is an environmentally friendly process, which gives high conversion without by-product formation and do not require recycling.[24] It has been reported that the solid-state reactions were usually carried out by mixing finely powdered reactants at room temperature and accelerated by heating, irradiation, or grinding, etc.[25]. In this work, heating and grinding methods were used and the temperature was set at 90°C (a little higher than the melting point of ligand **L)**. We monitored the progress of reaction by comparing the changes in melting peak area of remnant ligand **L** or resultant product in the mixtures using DSC. Figure 1 show one of the examples for the DSC curves of the reaction mixture of **L** and samarium chloride ($SmCl_3$ $7H_2O$) at various stages. The endotherm peak at approximate 85°C is characteristic for the melting of the ligand **L**, while another endotherm peak approximately located at 110°C could be associated with the resulting Sm complex. As shown in curve G15 in Figure 1, no endotherm peak of the product complex was observed for the mixture that was only ground for 15 min at room temperature. It is generally accepted that in a solid-state reaction the nucleus formation of product is essential to the yield of product.[24,26] As this process of nucleation was mainly controlled by temperature, a heating step is necessary for the reaction. After heated at 90°C for 120 min, the endothermal peak of the resultant complex appeared (in the curve G15H120), indicating that the temperature applied

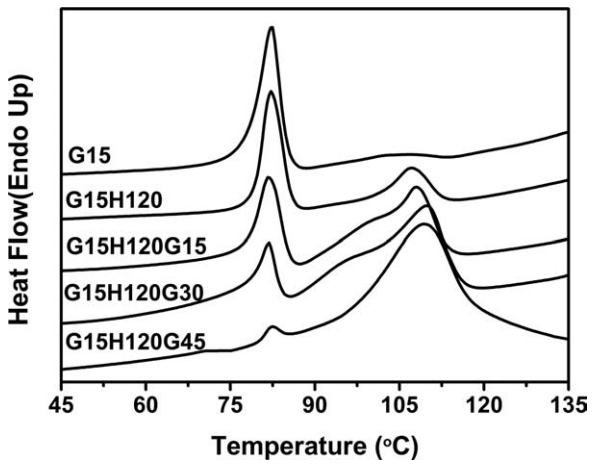

Figure 1 DSC curves of reaction mixture in different stages of solid-state reaction.

favors to the nucleation process. We found that the time of second grinding process after 120 min heating treatment is crucial for the reaction. From the DSC traces of mixture after further grinding 15, 30, and 45 min (curves G15H120G15, G15H120G30, and G15H120G45 in Figure 1, respectively), it can be found that the peak area of ligand **L** gradually decreases while the peak of product increases as the second grinding time increases. **L** had been nearly converted into complex when the mixture was ground for 45 min, as indicated by the absolutely dominant melting peak for complex and inferior melting peak for ligand **L** in the curve G15H120G45. After purification, the Sm complex was collected at a yield of 86%. All lanthanide complexes were synthesized using the identical G15H120G45 process with high yield (> 82%).

These synthesized complexes are insoluble in common solvents such as chloroform, DMF, DMSO, ethanol and MeCN. They have been characterized by elemental analysis, TGA and FTIR. The elemental analytical data for the complexes, presented in Table I, indicate that these lanthanide complexes conform to a 1 : 1 metal-to-ligand stoichiometry together with 2 mol H_2O, Ln**L**Cl_3 $2H_2O$.

The complexes have similar multistage thermal decomposition behaviors and their TGA results are summarized in Table II. All the samples have a weight loss from 90 to 180°C (Table II lists the fastest thermal decomposition temperature corresponding to the peak values in DTA endothermic curves). The weight loss in this temperature range is approximately equal to two water molecules, which is in agreement with the results determined by elemental analyses. The fact that the water molecule lost at a relatively low temperature (~118°C) suggests that the water is a crystal hydrate.[27] The complexes are stable up to 220°C and then decompose in the range between 220 and 700°C. Eventually, all the complexes are decomposed to their corresponding oxides (Ln_2O_3). The analysis of the thermogravimetric data supports the formula Ln**L**Cl_3 $2H_2O$ assigned for complexes on the basis of elemental analysis.

The FTIR spectra for the ligand L and a typical complex (La complex) are presented in Figure 2, with the position of their important infrared bands shown in Table III. Whereas the IR spectra of the complexes were similar due to their similar coordination structure, the comparison of these spectra with that of ligand **L** shows some important changes. The stretching vibration of the ν(C═O) shifts from 1720 cm^{-1} for ligand **L** to about 1732 cm^{-1} for the complexes ($\Delta\nu$ = 11–12 cm^{-1}), whereas the stretching vibration of the ν(C─O─C) at 1166 and 1218 cm^{-1} for ligand **L** remains approximately unchanged in the complexes. The band at 3320 cm^{-1} for free ligand assigned to the stretching vibration of the amine group ν(N─H) shifts to 3329–3334 cm^{-1} ($\Delta\nu$ = 9–14 cm^{-1}) in the complexes. Generally, coordinating to lanthanide ion should lengthen the C═O bond and shift the vibration ν(C═O) to a low frequency ($\Delta\nu = -10 \sim 30$ cm^{-1}),[28] which is opposite to the results observed in this work. We believe that this abnormal phenomenon is contributed from the hydrogen bonds formed between C═O and N−H group in free ligand, which will weaken the force constant of these bonds. This hydrogen bonds is thought to be broken in the coordination reaction, resulting in the blue shift of the band of ν(C═O) ($\Delta\nu$ = 40–60 cm^{-1}) and ν(N─H) to a higher frequency. Subsequently, after the C═O group coordinated to lanthanide ions, the ν(C═O) absorption band might

TABLE I
Elemental Analytical Data of the Lanthanide Complexes (%)

Complex	C found (calc.)	H found (calc.)	N found (calc.)	Ln found (calc.)
Y**L**Cl_3·$2H_2O$	46.73 (47.16)	8.30 (7.90)	3.81 (3.93)	12.90 (12.56)
La**L**Cl_3·$2H_2O$	46.10 (44.32)	7.56 (7.38)	3.72 (3.68)	18.22 (18.33)
Nd**L**Cl_3·$2H_2O$	42.99 (43.78)	7.44 (7.33)	3.42 (3.65)	18.42 (18.89)
Sm**L**Cl_3·$2H_2O$	42.32 (43.42)	7.93 (7.27)	3.47 (3.62)	20.52 (19.53)
Eu**L**Cl_3·$2H_2O$	42.47 (43.33)	8.02 (7.26)	3.46 (3.61)	19.18 (19.70)
Gd**L**Cl_3·$2H_2O$	42.42 (43.03)	7.92 (7.21)	3.44 (3.58)	19.41 (20.21)
Dy**L**Cl_3·$2H_2O$	41.63 (42.75)	7.74 (7.16)	3.41 (3.56)	20.35 (20.78)
Er**L**Cl_3·$2H_2O$	41.92 (42.49)	7.77 (7.12)	3.57 (3.54)	20.61 (21.26)

TABLE II
Thermo Analytical Data of the Lanthanide Complexes

Complex	The fastest H_2O loss temp. (°C)	Mass loss of H_2O (%)		Residue (%)		Residue product
		Found	Caculated	Found	Caculated	
Y**L**Cl_3 2H_2O	120.3	4.82	5.05	16.39	15.86	Y_2O_3
La**L**Cl_3 2H_2O	118.0	5.67	4.72	21.38	21.38	La_2O_3
Nd**L**Cl_3 2H_2O	117.6	4.32	4.69	21.49	21.89	Nd_2O_3
Sm**L**Cl_3 2H_2O	115.8	4.75	4.75	23.80	22.53	Sm_2O_3
Eu**L**Cl_3 2H_2O	113.0	5.02	4.64	22.21	22.69	Eu_2O_3
Gd**L**Cl_3 2H_2O	118.1	4.74	4.61	22.37	23.21	Gd_2O_3
Dy**L**Cl_3 2H_2O	116.8	5.09	4.58	23.35	23.73	Dy_2O_3
Er**L**Cl_3 2H_2O	120.1	4.31	4.56	23.57	24.19	Er_2O_3

shift to a lower frequency, which is even higher than its counterpart in the ligand.

In addition, some new bands appear in the spectra of the complexes. The band at 1600 cm^{-1} is related to the formation of the cheated ring >C=O···Ln—O or the N—H bending vibration. Furthermore, the broad band at about 3400 cm^{-1} can be attributed to the overlap of the asymmetric and symmetric H—O—H stretching vibrations in the water and the double multiple absorption of C=O and N—H.[29] The bands in the range of 540 to 595 cm^{-1} in different spectra of the complexes are also observed, which are associated with the Ln—O stretching vibrations.[30] These results together with the elemental and TGA data suggest that the Ln is most probably coordinated by two oxygen atoms at the carbonyl group in ligand **L**.

Photostabilizing efficiency

The photostabilizing efficiency of synthesized complexes and ligand L in PP was studied using FTIR and TGA. The main photodegradation products of PP include hydroperoxides and carbonyls, such as carboxylic acids, ketones, and lactones, which show apparent absorption between 1700 and 1800 cm^{-1} in FTIR spectra of aged PP films. Therefore, the photodegradation extent of PP can be easily characterized by CI calculated as the area of carbonyl absorption band related to the area of a reference band at 2700 to 2750 cm^{-1}.[23] Figure 3(a) shows the CI values of unstabilized PP film, PP films stabilized with ligand **L** and various lanthanide complexes at different UV irradiation time. It should be noted that CI changes for all these samples have similar tendency. The CI values are already evident after a short (6–8 days) irradiation and are gradually enhanced with the exposure time increasing. However, the CI curves of the stabilized samples, which overlap more or less in a narrow region without distinct difference, are evidently lower than that of unstabilized PP at prolonged irradiation time (i.e. 8 days later). These results suggest that the lanthanide complexes have comparable photostabilizing efficiency compared to the HALS ligand **L**.

To compare the photostabilizing efficiency of ligand **L** and the complexes, we calculated the differences (ΔCI) between the CI of stabilized samples and that of unstabilized PP at the same UV irradiation time. The results are shown in Figure 3(b). It could be found that the photostabilizing efficiency of the complexes are dependent on the kind of lanthanide iron: the Nd, Dy, Er, and Sm complexes are more effective than ligand **L**, while the Gd, La, Y, and Eu complexes are not as effective as ligand **L**. Among these complexes, the Nd complexes have the

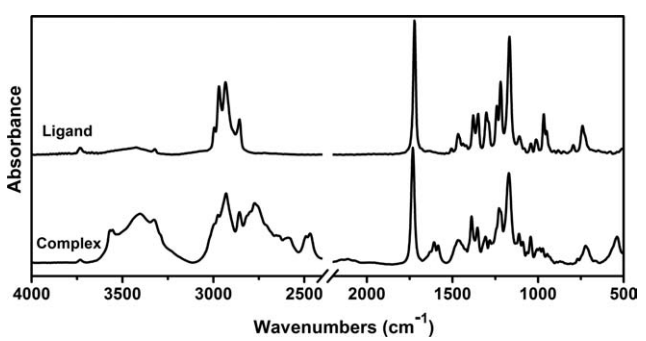

Figure 2 The FTIR spectra of ligand **L** and La complex.

TABLE III
Position of Some Main IR Bands of the Ligand L and its Complexes (cm^{-1})

Compounds	ν(C=O)	ν(C—O—C)	ν(N—H)	ν(Ln—O)
L	1720	1166, 1218	3320	
Y**L**Cl_3·2H_2O	1732	1169, 1215	3330	542
La**L**Cl_3·2H_2O	1732	1169, 1216	3332	545
Nd**L**Cl_3·2H_2O	1732	1172, 1215	3329	566
Sm**L**Cl_3·2H_2O	1731	1173, 1214	3333	576
Eu**L**Cl_3·2H_2O	1732	1172, 1215	3331	584
Gd**L**Cl_3·2H_2O	1732	1168, 1215	3334	546
Dy**L**Cl_3·2H_2O	1731	1169, 1216	3333	565
Er**L**Cl_3·2H_2O	1732	1169, 1215	3332	541

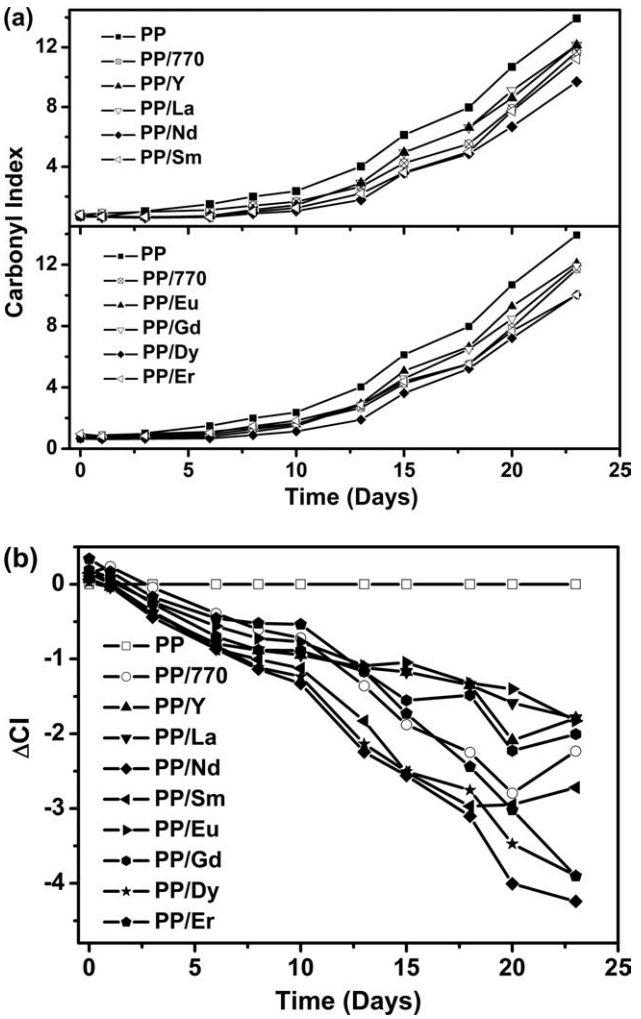

Figure 3 The plots of carbonyl index (a) and ΔCI (b) versus irradiation time for various PP samples (PP/770 and PP/Ln represent PP samples containing 0.5 wt % of ligand **L** and Ln complex, respectively).

best photostabilizing performance. After 23 days of UV irradiation, the CI value for PP/Nd is 9.7, which is much lower than that for PP/**L** of 11.7 or unstabilized PP of 13.9, respectively.

It has been reported that thermal decomposition temperatures of PP samples can be reduced under UV irradiation due to photodegradation.[31] Thus, thermal stability of irradiated samples can be used to evaluate the effect of stabilizer on sample photostability. In this contribution, the temperatures at 5% weight loss ($T_{-5\%}$) were determined from the TGA curves (Fig. 4**)** of unstabilized and stabilized PP samples after 25 days UV irradiation and used to compare the stability of various PP samples, as listed in Table IV. After 25 days UV irradiation, the $T_{-5\%}$ values of the stabilized samples are about 8.0–25.6°C higher than unstabilized PP. For these stabilized samples, decomposition onset for UV-PP/**L** occurs later than UV-PP/Gd, UV-PP/La, UV-PP/Y, and UV-PP/Eu, but earlier than UV-PP/Nd, UV-PP/Sm,

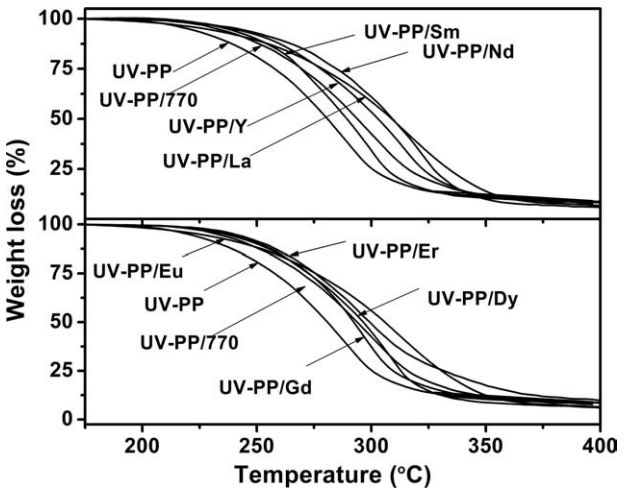

Figure 4 TG trace of the PP samples after 25 days of UV irradiation (PP/770 and PP/Ln represent PP samples containing 0.5 wt % of ligand **L** and Ln complex, respectively).

UV-PP/Er, and UV-PP/Dy. Among all the samples, UV-PP/Nd has the highest $T_{-5\%}$ value of 239.6°C. These results match well with CI tendency measured with FTIR.

Figure 5 shows the changes in elongation at break of neat PP, PP/770, and PP/Nd samples with UV irradiation times. It should be noted that the elongation for all samples have similar tendency of sharply decrease with increasing of irradiation times. Without UV irradiation, they have similar initial values of elongation at break: 21.7, 21.1, and 22.4% for neat PP, PP/770, and PP/Nd respectively, which suggests that the introduction of ligand **L** and Nd complex has negligible effect on the initial tensile properties of PP. However, after UV irradiated for 48 h, the elongation at break decreased to 3.7% for neat PP, while that value became 5.4% and 9.9% for PP/770 and PP/Nd, respectively. The tensile results indicate that the Nd complex has improved photostabilizing performance than ligand **L**, which is

TABLE IV
$T_{-5\%}$ of Various PP Films Underwent 25 Days UV irradiation, as well as Underwent 48 h Extraction and 18 Days UV Irradiation (°C)

Samples	25 Days UV irradiation	48 h Extraction and 18 days UV irradiation
PP	214.0	238.0
PP/**L**	228.3	242.3
PP/Y	227.2	245.2
PP/La	224.2	251.3
PP/Nd	239.6	259.0
PP/Sm	234.0	253.6
PP/Eu	222.0	254.2
PP/Gd	228.9	252.6
PP/Dy	229.3	246.9
PP/Er	232.5	248.4

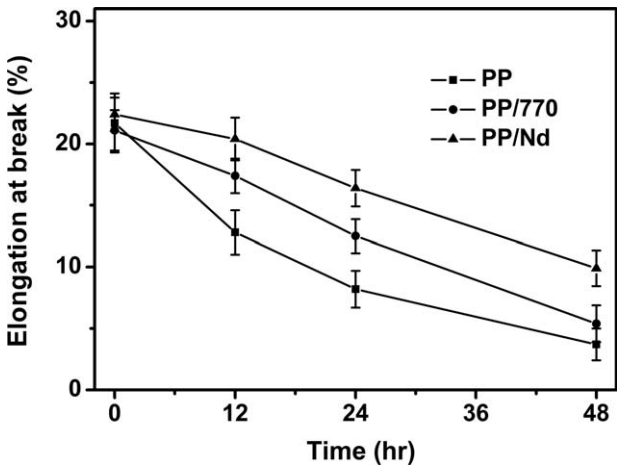

Figure 5 The plots of elongation at break versus irradiation time for PP, PP/770, and PP/Nd (PP/770 and PP/Nd represent PP samples containing 0.5 wt% of ligand **L** and Nd complex, respectively).

consistent with the measurements of carbonyl index and thermal decomposition temperature.

The ligand **L** is an effective commercial photostabilizer for polymers. Therefore it is easily presumed that **L**-based complexes have effective photostabilizing efficiency as well. In addition, it can be suggested that lanthanide ions also act important roles in the photostabilization process, which is associated with the fact that the efficiency of the complexes depend on the kind of rare earth. It has been reported that some lanthanide complexes were better inhibitor for $O_2^{-\bullet}$ than that of the nitroxyl tempo >NO·, which is the functional derivative of >NH, and had significant scavenging activity of superoxide radical.[20] At this stage of our research the detailed mechanism of lanthanide complexes in stabilizing polymer is completely unknown. On the other hand, as proposed by Audouin[32] and Kotek,[33] the crystalline morphology of a semicrystalline polypropylene greatly affects its photodegradation behavior. However, by carefully investigating using WAXD and DSC, we found that there is no obvious difference in the crystallization behavior and phase morphology among these samples of pristine PP, PP/L, and various PP/Ln. Therefore, the **L** or Ln complexes addition favors the photostabilizing of PP by changing its crystalline morphology should not be an important contributory mechanism. The detailed mechanism is worthy for further investigation.

Solvent-extraction resistance

A stabilizer loses its efficiency in polymer mainly due to oxidation and migration. The loss of stabilizer by physical migration is even significantly larger than the fraction lost by oxidation in some case.[34] Therefore, in addition to the photostabilizing efficiency, the solvent-extraction resistance is also a very desirable property in practical applications of a stabilizer. As potential light stabilizers, the extraction resistance of these lanthanide complexes was determined by ethanol extraction. PP samples were extracted with ethanol solution and subsequently irradiated by UV light. Figure 6(a,b) show the plots of CI and ΔCI values versus the irradiation time, respectively, for ethanol extracted samples. After extraction, the CI values of PP samples rise quickly, which may be due to the loss of stabilizers during solvent extraction. For example, after 15 days of UV irradiation, CI values of unextracted PP/**L** and PP/Nd are 4.2 and 3.6, respectively (Fig. 3), while the CI values of the corresponding extracted samples become 10.2 and 8.2, respectively (Fig. 6). It is also observed that those extracted samples become completely fragile after only 18 days of photo-oxidation, which is much earlier than unextracted samples (25 days).

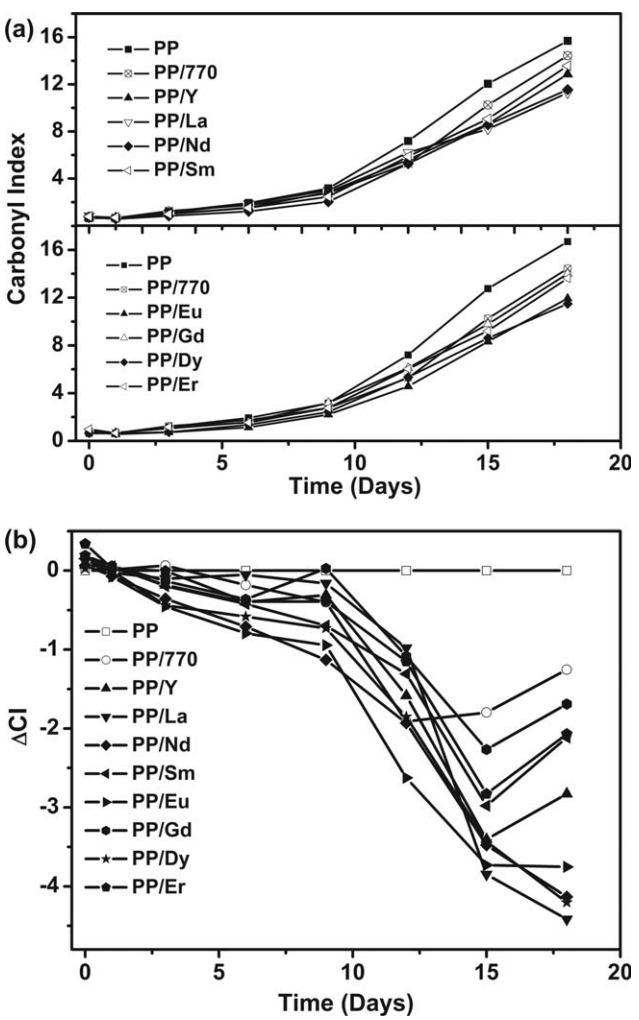

Figure 6 The plots of carbonyl index (a) and ΔCI (b) *versus* irradiation time for extracted PP samples (PP/770 and PP/Ln represent PP samples containing 0.5 wt % of ligand L and Ln complex, respectively).

As has been demonstrated in section of **3.2** that, among these complexes, the Nd, Dy, Er, and Sm complexes were more effective, whereas the Gd, La, Y, and Eu complexes were not as effective as ligand **L** in PP photostabilization efficiency. Interestingly, for these extracted samples, all the complexes-stabilized PP films, as revealed in Figure 6(b), clearly show lower CI values than PP/**L** after a long period of UV irradiation (more than 12 days). These results reveal that lanthanide complexes-stabilized PP samples are more stable than ligand **L**-stabilized sample during solvent extraction, which suggests that these complexes have better extraction resistance than ligand **L**.

The values of $T_{-5\%}$ for the extracted samples after 18 days of UV irradiation are also measured and listed in Table IV. All of the stabilized samples have higher $T_{-5\%}$ values than the unstabilized PP. The $T_{-5\%}$ value of PP/**L** is 4.3°C higher than that of unstabilized PP. In contrast, the $T_{-5\%}$ values are improved remarkably for the complexes-stabilized samples, which are 7.2–21.0°C higher. Among these complexes-stabilized samples, the PP/Nd has the highest $T_{-5\%}$ of 259.0°C, which is 21.0°C and 16.7°C higher than that of unstabilized PP and PP/**L**, respectively. These thermal analysis results also reveal that the complexes-stabilized samples are more stable than ligand **L**-stabilized sample at long-term photodegradation after extraction.

The accurate reason why solvent-extraction resistance of ligand **L** is improved by forming its complexes with lanthanide ions is still unclear. It might be related to higher molecular weight of the complexes as well as possible interaction between lanthanide ions and the preoxidized polymer chains. It is well known that the volatility and diffusion rate of light stabilizers would be simultaneously decreased with the increasing of the molecular weight.[7] In the complexes with stoichiometry formula of $Ln\mathbf{L}Cl_3\ 2H_2O$, lanthanide irons act as bridge to connect ligand molecules, which increases the molecular weight and consequently improves the migration resistance. Moreover, it is possible that lanthanide ions interact with carbonyl products and acyl macroradicals on polymer chain, which are generated during the photo-oxidation of PP.

CONCLUSIONS

We have succeeded in preparing a series of lanthanide complexes (Nd, Dy, Er, Sm, Gd, La, Y, and Eu) with a low molecular weight HALS Tinuvin 770 for the first time via a simply solvent-free solid-state reaction. In the complexes, lanthanide ions are coordinated with C=O oxygen atoms of the ligand **L**. These complexes have better solvent-extraction resistance than ligand **L** and their photostabilizing efficiencies are dependent on the kind of lanthanide ions: the Nd, Dy, Er, and Sm complexes are more efficient than ligand **L**. Although the detailed mechanism of lanthanide complexes in stabilizing polymer needs further investigation, our preliminary results suggest that it is possible to prepare lanthanide complexes with simultaneously improved photostabilizing efficiency and extraction resistance by optimizing specific lanthanide ions and HALS ligands. Considering the simple solvent-free synthesis process and the fact that most of light rare earth compounds are much cheaper than common HALS, this study suggests a potential environmental-friendly technique for achieving cheap and efficient light stabilizers for polymer.

References

1. Laura, C. D.; Robert, W. M. Characterization of Weather Aging and Radiation Susceptibility, Engineering Plastics; ASM International: Ohio, 1988; Vol. 2, p 575.
2. Pearce, E., Ed. Photodegradation, Photo-oxidation and Photostabilization of Polymers; Wiley-Interscience: New York, 1975; Chapter 3.
3. Gugumus, F. Polym Degrad Stab 1993, 40, 167.
4. Klemchuk, P. P.; Gande, M. E. Polym Degrad Stab 1988, 22, 241.
5. Step, E. N.; Turro, N. J.; Gande, M. E.; Klemchuk, P. P. Macromolecules 1994, 27, 2529.
6. Wilén, C. E.; Auer, M.; Stranden, J.; Näsman, J. H.; Rotzinger, B.; Steinmann, A.; King, R. E.; Zweifel, H.; Drewes, R. Macromolecules 2000, 33, 5011.
7. Gugumus, F. Polym Degrad Stab 1999, 66, 133.
8. Pospíšil, J.; Pilař, J.; Nešpůrek, S. J Vinyl Addit Technol 2007, 13, 119.
9. Al-Malaika, S. Adv Polym Sci 2004, 169, 121.
10. Minagawa, M. Polym Degrad Stab 1989, 25, 121.
11. Pan, J. Q.; Lau, W. W. Y.; Lin, J.; Tan, K. L. Polym Degrad Stab 1994, 46, 51.
12. Auer, M.; Nicolas, R.; Rosling, A.; Wilén, C. E. Macromolecules 2003, 36, 8346.
13. Ekman, K.; Ekholm, L.; Näsman, J. H. J Polym Sci Part A: Polym Chem 1995, 33, 2699.
14. Mosnáček, J.; Bertoldo, M.; Kósa, C.; Cappelli, C.; Ruggeri, G.; Lukáč, I.; Ciardelli, F. Polym Degrad Stab 2007, 92, 849.
15. Ling, Q. D.; Kang, E. T.; Neoh, K. G.; Huang, W. Macromolecules 2003, 36, 6995.
16. Poole, R. A.; Montgomery, C. P.; New, E. J.; Congreve, A.; Parker, D.; Bottab, M. Org Biomol Chem 2007, 5, 2055.
17. Lauffer, R. B. Chem Rev 1987, 87, 901.
18. Su, Q. D.; Mao, J. J.; Zhao, G. W.; Zhang, M. S. J Mol Struct 1997, 403, 231.
19. Chen, J. P.; Patil, S.; Seal, S.; McGinnis, J. F. Nat Nanotechnol 2006, 1, 142.
20. Wang, B. D.; Yang, Z. Y.; Li, T. R. Bioorg Med Chem 2006, 14, 6012.
21. Zhou, J.; Wang, L. F.; Wang, J. Y.; Tang, N. J Inorg Biochem 2001, 83, 41.
22. Li, Y. H.; Yang, Z. Y.; Wang, B. D. Transit Met Chem 2006, 31, 598.
23. Rabello, M. S.; White, J. R. Polym Degrad Stab 1997, 56, 55.
24. Xin, X. Q.; Zheng, L. M. J Solid State Chem 1993, 106, 451.

25. Toda, F. Acc Chem Res 1995, 28, 480.
26. Jacobs, P. W. M.; Tompkins, F. C. Chemistry of the Solid State; Butterworth: London, 1955.
27. Woźnicka, E.; Kopacz, M.; Umbreit, M.; Kłos, J. J Inorg Biochem 2007, 101, 774.
28. Robert, M. S.; Francis, X. W.; David, K. Spectrometric Identification of Organic Compounds; John Wiley & Sons, Inc.: New York, 1974.
29. Yan, B.; Qiao, X. F. J Phys Chem B 2007, 111, 12362.
30. Moeller, T. Gmelin Handbook of Inorganic Chemistry; Springer-Verlag: New York, 1981.
31. Zhao, H. X.; Li, R. K. Y. Polymer 2006, 47, 3207.
32. Audouin, L.; Langlois, V.; Verdu, J.; Debruijn, J. C. M. J Mater Sci 1994, 29, 569.
33. Kotek, J.; Keinar, I.; Baldrian, J.; Raab, M. Eur Polym J 2004, 40, 2731.
34. Lundbäck, M.; Hedenqvist, M. S.; Mattozzi, A.; Gedde, U. W. Polym Degrad Stab 2006, 91, 1571.